

Visible Light Knows Who You Are

Chuankai An, Tianxing Li, Zhao Tian, Andrew T. Campbell, and Xia Zhou
Department of Computer Science, Dartmouth College
{chuankai, tianxing, tianzhao, campbell, xia}@cs.dartmouth.edu

ABSTRACT

We examine the feasibility of human identification using purely the ubiquitous visible light. Empowered by the Visible Light Communication (VLC), the identification system consists of VLC-enabled LED lights on the ceiling emitting light beacons, and photodiodes on the floor capturing a continuous stream of shadow maps each corresponding to an LED light. We leverage these shadow maps to localize a user's key body joints in the 3D space and recognize the user based on the estimated body parameters (e.g., shoulder width, arm length). Preliminary results with 10 participants show 80% success rate, i.e., correctly identifying 8 participants out of 10. The mean error of the body parameter estimation is 0.03 m. To extend the system to diverse practical settings, we discuss our plan of incorporating advanced behavioral features to enhance the identification accuracy and robustness.

Categories and Subject Descriptors

C.2.1 [Network Architecture and Design]: Wireless communication

Keywords

Visible light communication; Human identification

1. INTRODUCTION

Human identification is of great interests to a variety of applications. Recognizing who we are is crucial for user authentication. Applications running on smart devices (e.g., smartphones, smart watches) can provide personalized services (e.g., sending personalized notifications) and customize system configurations based on the user identity. Smart spaces can adapt its environmental settings based on a user's preferences. Imagine a user walking into a room. The environment immediately recognizes the user and controls the ambient smart devices to adapt the room settings (e.g., temperature, light) tailored to meet this user's needs.

Existing technologies available for human identification, however, have been very limited. We divide them into two categories.

The first category of methods require users to constantly wear on-body sensors or devices (e.g., bioimpedance sensors [4], ultrasonic sensors [27]). These sensors or devices continuously measure user's biometric features or behavioral information and leverage the information to recognize users. Carrying the sensors and devices all the time, however, is burdensome to users, preventing these methods from a wide adoption. The second category of methods [3, 13] rely on cameras to capture video frames and extract user features (e.g., facial features, gait) from the image frames to identify users. However, cameras are high-fidelity sensors. Capturing raw image data using cameras inevitably brings privacy concerns. Even worse, the sensitive image data can fall into the hands of the adversary [24, 35]. Recent work has examined the use of RF signals to track users [1, 5, 14, 23, 34], yet only at the level of recognizing user gestures and activities, rather than differentiating users.

To address the above limitations, in this paper, we seek a different approach to human identification. In particular, we examine the feasibility of using the ubiquitous light around us to recognize who we are, without requiring users to carry any on-body devices, neither using any cameras constantly monitoring users. The idea of light-based human identification is enabled by the recent advances in Visible Light Communication (VLC) [16, 28]. VLC encodes data into light intensity changes imperceptible to human eyes, and any devices equipped with light sensors (photodiodes) can detect the light change and decode data. Human identification using visible light is part of the vision of integrating communication and sensing into the ubiquitous light [38].

The light-based human identification system consists of VLC-enabled LED lights on the ceiling, and photodiodes embedded on the floor¹. Each LED light actively transmits data using VLC to smart devices in the room. More importantly, leveraging a recent technique proposed in [19], each LED light also periodically emits light beacons (i.e., flashing at a unique frequency) using VLC. Photodiodes transform the perceived light intensity values over time to the frequency domain, separate the light rays coming from individual light sources, and recover the shadow maps cast by the human body in the presence of each single light. By examining the shadow maps cast in different directions, we can extract key body features (e.g., shoulder width, arm length) of individual users. By analyzing the continuous shadow maps over time, we can further learn user's behavioral and movement characteristics. These body features and movement characteristics serve as the basis for the system to differentiate users.

To realize light-based human identification, the key challenge we face lies in dealing with the low-resolution, binary shadow maps

Permission to make digital or hard copies of all or part of this work for personal or classroom use is granted without fee provided that copies are not made or distributed for profit or commercial advantage and that copies bear this notice and the full citation on the first page. Copyrights for components of this work owned by others than ACM must be honored. Abstracting with credit is permitted. To copy otherwise, or republish, to post on servers or to redistribute to lists, requires prior specific permission and/or a fee. Request permissions from Permissions@acm.org.

VLC'15, September 11, 2015, Paris, France.

© 2015 ACM. ISBN 978-1-4503-3702-1/15/09 ...\$15.00.

DOI: <http://dx.doi.org/10.1145/2801073.2801078>.

¹Engineering photodiodes on the floor can be eased with the advent of smart textile [22], which can integrate photodiodes into the rugs, carpet, and sofa.

recovered by the photodiodes. Constrained by the photodiode density, these shadow maps contain much fewer pixels than camera image frames, which consist of at least tens of thousands of pixels. Furthermore, image frames contain additional information such as color, brightness contrast, and texture. As a result, to extract body features from the recovered shadow maps, existing computer vision algorithms can not be directly applied, as they are all designed for processing the image frames with a much higher resolution.

In this work, we take initial steps to tackle the above challenge, working towards realizing human identification using the visible light. We examine approaches to extracting body features from low-resolution, binary shadow maps. We design a lightweight classifier that can distinguish users on the fly. We implement our system in a $3\text{ m} \times 3\text{ m}$ testbed, with 324 photodiodes on the floor and 5 LED lights on the ceiling. Initial results with ten participants show that our current algorithms achieve 80% success rate and 0.08 m estimation error of key body parameters. These results demonstrate the feasibility of our approach, yet also point out a number of open research questions that we need to further address. We conclude by discussing our plan to boost the identification accuracy and robustness in practical settings.

2. SYSTEM OVERVIEW

We first introduce the goal and framework of the VLC identification system. We aim to overcome the challenge of shadow maps' low resolution, which limits the number of features we can extract. Overall, the system identifies a user based on the shadow maps currently recovered. As the user steps into the system, the system gathers signals from photodiodes embedded in the floor, infers shadows cast by individual light sources, and outputs the identification result. That is, whether this is a new user or this user has been here before. The system either assigns a new ID to the user or links the user to an existing ID.

For the system to work, LED lights on the ceiling are transmitters and light sensors on the floor are receivers. Using the technique in [19], each LED light is instrumented to emit periodical light beacons (i.e., flashing at a unique frequency) while providing networking connectivity to smart devices in the environment. When LED lights cast shadow on the floor with modulated light beams, the light sensors record the light intensity at different locations. The perceived light intensity at each light sensor is the summation of all unblocked light rays from LED lights to the light sensor. The light intensity data is then transformed to the frequency domain for the light sensor to separate the light rays from different light sources. By tracking the frequency power change over time and aggregating the data from all light sensors, we can recover the shadow map corresponding to each single light.

Given shadow maps of LED lights from different angles, we can localize several key points on body in 3D space since human body shadows have special patterns. The principle is simple: when a point on body blocks two light beams from different angles, if we find the two light beams, the intersection of two beams should be the point we need to localize on the body.

Once we localize the key joints of the user body, we can infer several body features such as shoulder height and shoulder width. They describe a body figure from different angles. In addition, by analyzing user's shadow maps continuously over time, we can infer user's behavioral patterns (e.g., gait) by tracking the locations of key points. Combining the behavioral patterns with the static body features can allow finer-grained user identification. After obtaining a vector of features on body parameters and behavioral patterns, we can build classifiers to classify users in real time. The system can recognize whether the current person has been seen before or this

is a new user. In the next two sections, we describe two key steps (obtaining shadow maps and user identification) in detail.

3. OBTAINING SHADOW MAPS

We now describe how to collect shadow maps for each light source based on a recent work [19].

VLC Link. As a standard indoor VLC system, a one-way VLC link includes three components, transmitter, receiver, and the attached device to collect data from receivers. We mount five common LED lights on the ceiling as transmitters. Each LED light has one additional Arduino UNO board to control the Pulse Width Modulation (PWM) frequency of light beacons, so that the LED lights can send out information in the form of light-on and light-off. Human eyes cannot perceive the light pulse since it is set from 1.6 to 3.4 KHz. We choose different high frequencies to avoid the flickering problem [17] and there is an interval between any two selected frequencies so that it is easy to separate signals without interference. The receivers are photodiodes on the floor, which can sense the light intensity at their locations. We connect several photodiodes to a Arduino board. Different light intensity correspond to the voltage reading on Arduino board. Finally, all Arduino boards are connected together to a server.

Signal Processing. We obtain a series of voltage readings of each photodiode. The readings reflect the sum of light intensity at the location of photodiode. If all lights are flashing with different pulse frequencies, we can separate them using Discrete Fourier Transform (DFT), which transforms the received light intensity series from the time domain to the frequency domain. In the frequency domain, if a light is unblocked, we can detect a pulse near its modulation frequency. When the light beam is blocked by human body, the existing pulse will disappear in frequency domain. That is, by detecting the change in frequency domain, for each pair of LED light and photodiode on the floor, the system will know whether the light beam is blocked. We combine the result of all photodiodes to derive a binary shadow map for each LED light. Here we deploy 18×18 photodiodes on the floor, so each shadow map has 324 pixels to show human body shadow from different angles. Based on shadow maps, we can extract personal features for human identification.

4. EXTRACTING FEATURES AND IDENTIFYING USERS

We next illustrate how to estimate body parameters using the captured shadow maps. We also discuss potential solutions to deriving more behavioral and dynamic features, such as gait. We then design a classifier using the nearest neighbor method to classify users on the fly.

Patterns in Shadow Maps. Our design is driven by the observation that shadows cast by users with different body figures exhibit different features. In Figure 1(a), each row contains a user's five shadow maps from the front, top, back, right and left LED lights using our testbed (Section 5). The shadow map resolution is 18×18 since each light sensor on the floor contributes the status of one pixel on the shadow map. Here a black pixel means a blocked light sensor. Figure 1(a) illustrates the posture of the two users. Even on these low-resolution shadow maps, we can see the difference the two users, which is the basis for us to extract suitable features. If a user holds right arm towards front and right horizontally, and left arm towards front and left horizontally as Figure 1(b), five shadow maps from different angles illustrate the body shape.

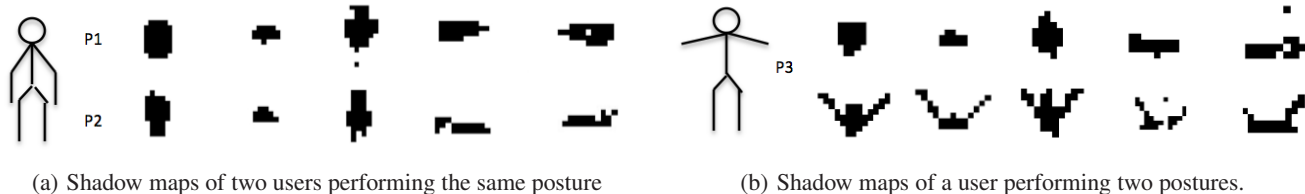


Figure 1: Shadow maps of three users under five LED lights, located on the front, top, back, right and left with respect to the user.

From the shadow maps in the middle column of Figure 1(a), we can see several body parts. The upper large square represents head, the left vertical blocks are like an arm, the middle area is the shadow of torso, and one leg projects its shadow to the lower left slim rectangle on the map. Since light sensors are sparse on the floor, projection of the right leg may be located between light sensors so that right leg does not have a projection on the shadow map. In Figure 1(a), the shadow from top light does not offer much information except the size and shape of body, but the top light shadow is meaningful if the person has a moving body part which is not attached to body. When a person stretches out two arms as Figure 1(b), from back and front angle, we can clearly see the dense pixels in the middle of torso and two series of blocks on both sides as two arms.

Feature Extraction. We take shoulder height and shoulder width as examples to show how to extract features of body figure, since the shadow of tall people exceeds the edge of testbed, and sometimes arms are attached to the torso so that it is difficult to estimate the width of torso only.

The inputs are shadow maps from all light sources in a period of time, when a user is walking on the testbed. We can localize both shoulders on a shadow map based on the following pattern. The projection of left/right shoulder will be in the most left/right column from the front or back angle in Figure 1. In that column, shoulder should be in the farthest row from the light source. Here are several key steps.

#1: Select shadow maps. The light source in front of or behind a user can project shoulders more clearly on the floor than the light sources on the left/right side, so we compute the user’s orientation based on the change of user’s location in consecutive maps. If the direction from light source to shadow’s centroid is close to user’s orientation, the shadow map of that light source is a good choice. Here we need two shadow maps for the following operations.

#2: Rotate maps. Shadow map consists of several discrete points, so we can apply Principal Component Analysis (PCA) to get the principal component of shadow. It looks like the axis of symmetry on human body. If it is not parallel to the y axis of light sensor array, rotate some angle depends on the principle component so as to achieve an upright shadow, such as the examples in Figure 2(a).

#3: Find projections using histogram. First, draw a histogram of points in the shadow. In Figure 2(b), x axis shows the column of points, y axis reflects the number of points in each interval on x axis. Torso, head and legs cover more points in the middle than two arms on both sides, so by detecting the change of height in the histogram, we can locate the column of each shoulder’s projections. The furthest point from light source in that column should be the projection of the shoulder. Since points in a shadow map are discrete, we adjust half unit in both x and y direction on the index of projection.

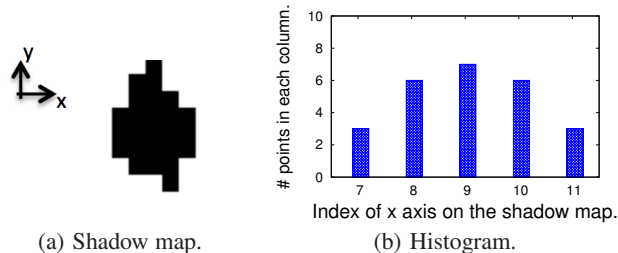


Figure 2: The histogram of a shadow map.

#4: Intersect light rays. Once we know the projection of left/right shoulder in two shadow maps, we connect the projection to the corresponding light source to obtain two light rays. The intersection of these two light rays should be the location of left/right shoulder in space. If they do not intersect, the location of shoulder is the midpoint of the segment which has the minimum distance between those two light rays. When we know the locations of both shoulders, we also get the shoulder width and shoulder height. We can filter the incomplete or noisy shadow maps, and compute the average values using the other shadow maps to improve the accuracy. If a user has more static gestures such as waving arms, more body features are available using the above method. For example, if we can localize the elbow by a waving arm, we can derive the length of the upper arm.

Furthermore, when users can walk freely on the testbed, the VLC system can provide more behavioral features such as gait. These behavioral patterns are valuable especially when the body features are not enough to distinguish a group of users. Since the sampling rate for shadow map is 60 Hz, a time series of shadow maps can reflect the subtle differences between frames of a movement. It is feasible to obtain the magnitude of the user stride and the walking speed by the analyzing changes in consecutive shadow maps.

Classification. In this paper, we classify a user using a simple nearest neighbor method. We select two sample body parameters as the features in our initial design. We initialize the set of recognized user IDs as an empty set. As users enter our system one by one, the system captures shadow maps for each light source, extracts features, compares features of the current user with the features of users who have been identified before, and determines whether the current person has been identified or the person is a new user with a threshold. When more body and behavioral features are measured, we plan to explore more advanced classifier designs.

5. EVALUATION

We next present details of our experiment setting and evaluate the accuracy of the body parameter estimation and user identification.

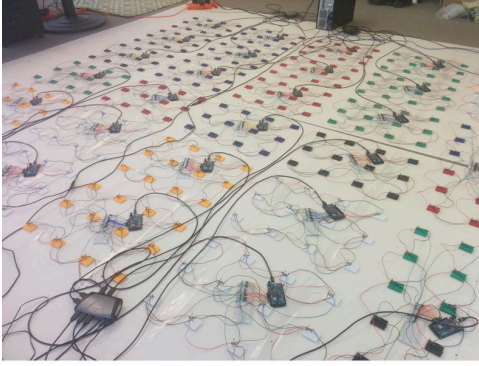


Figure 3: The array of light sensors on the floor.

Table 1: Measured features of participants (m).

Feature ID	1	2	3	4	5
Shoulder_h	1.58	1.54	1.45	1.39	1.60
Shoulder_w	0.47	0.36	0.38	0.42	0.46
Arm_l	0.69	0.70	0.59	0.60	0.64
Upper arm_l	0.33	0.36	0.28	0.30	0.27
Feature ID	6	7	8	9	10
Shoulder_h	1.48	1.44	1.27	1.39	1.44
Shoulder_w	0.41	0.39	0.42	0.44	0.43
Arm_l	0.62	0.61	0.56	0.56	0.63
Upper arm_l	0.27	0.27	0.24	0.24	0.29

Testbed. The testbed covers $3\text{ m} \times 3\text{ m}$ on the floor with 18×18 light sensors as Figure 3. The light sensors are deployed in a square array, the distance between two adjacent light sensors is 0.166 m. 27 Arduino boards collect the light intensity data from all light sensors (Honeywell SD3410) with a sampling rate of 60 Hz. The height of ceiling is 2.65 m, on which there are five LED lights (Cree CXA25) in cross shape. The middle one is above the center of testbed. The distance between the middle LED light to another is 0.8 m. More details about the testbed are in [19].

Participants. We invite 10 users with diverse body shapes as the test users. They move randomly in the testbed yet carefully to avoid sensors and boards on the floor. They also stay in several static postures, such as standing (Figure 1(a)), folding arms with two elbows pointing to the left and right, and stretching out two arms towards right-front and left-front respectively as Figure 1(b). Since devices are exposed to space, users movement are restricted, especially for legs. We ask participants to only move arms freely. Among the ten participants, seven are male and three are female. The range of age is from 20 to 31. Their height is from 1.55 m to 1.90 m. The weight is from 45 kg to 87 kg. Table 1 shows body features of the participants, which are shoulder height, shoulder width, arm length and upper arm length.

Body Feature Estimation. We choose shoulder height and shoulder width as two features to classify people. We estimate features in the following three settings due to real testbed conditions.

First, users are standing in the middle of the testbed with static postures and fixed orientation towards the light in front. When they are standing as Figure 1(a), the problem of finding projections is simple since we do not rotate the map. Figure 4 shows the mean error of shoulder height is 0.028 m and the mean error of shoulder width is 0.032 m for 10 participants. We also estimate two more body figures with the other static postures, the mean error of arm length is 0.028 m and that of upper arm is 0.036 m.

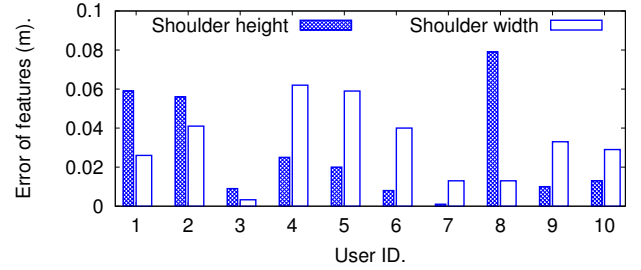


Figure 4: The error between estimated body figures and the ground truth of 10 participants in static standing.

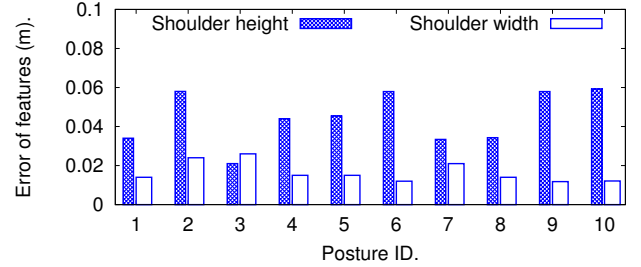


Figure 5: The error between estimated body figures and the ground truth of one participant in 10 movements.

Second, we ask the user with the ID of 1 to move arms randomly in 10 different meaningful movements, such as waving hands and opening a door. Each movement generates 550 consecutive groups of shadow maps in about 9 seconds. Each group contains 5 shadow maps from all LED lights. However, users still stand in the middle of testbed with fixed orientation. The error of shoulder height is 0.044 m and the error of shoulder width is 0.016 m for the user's 10 movements as Figure 5, which are slightly smaller than the user's errors in the first case. It supports that the multiple shadow maps in dynamic movements work better than maps of a static posture.

Third, users can walk on the testbed with free arms, so the orientation is not fixed. However, because of the dense deployment of exposed devices, users cannot walk freely. It is not the case when we can estimate orientation by user locations in consecutive shadow maps. We select 22 time slots in equal interval among 550 groups of shadow maps. The orientation at each time slot is manually labeled from 8 kinds of directions (right, right front, front, left front, left, left back, back and right back). Figure 6 reflects errors of 6 participants. The average error of shoulder height is 0.0278 m and that of shoulder width is 0.031 m.

The high accuracy of body figure estimation proves the feasibility and availability of methods in Section 4, though we have different assumptions in the above three cases. However, several factors limit the accuracy. The first factor is the low resolution of shadow map since the interval between light sensors on the floor results in the uncertainty in searching of projections. The second factor is the number of LED lights on the ceiling. If more LED lights cast light rays from different angles, we have more choices when selecting shadow maps. For the third case of dynamic movement, users look down at floor to avoid treading devices, which weakens the pattern in shadow histogram. The labeled orientation is not very accurate, which disturbs the selection of best shadow maps with the pattern of shoulders.

Classification. Since the mean error of body feature estimation is about 0.03 m, the threshold in the classification algorithm is set as

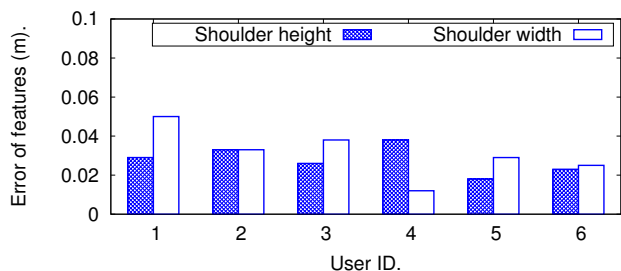


Figure 6: The errors of two features when users are moving steps on the testbed with exposed devices.

0.03 for all features, which determines whether body figures of two people are similar enough. When 10 users are entering the testbed in a random order, the identification accuracy using shadow maps of static standing is 80%, since the user pair (4, 9) and the user pair (3, 7) have a very similar body figures shown in Table 1. Among 45 different pairs in 10 people, the two pairs have a minor difference in the ground truth of shoulder height and shoulder width. This indicates that the gap of shoulder height or shoulder width is less than 0.02 m. For a user pair, if the gap of shoulder height or shoulder width is larger than 0.02 m, the classification can distinguish the two users. Current experiment shows that the granularity of VLC identification system is 0.02 m. The granularity can vary depending on the body shape of the participants and their movement types. We plan to go beyond static body features and incorporate movement characteristics [3, 12, 31, 32, 33] as our future work.

We also compare the result with the other methods. For example, in [7], the accuracy of identification using infrared sensors is 78.5% or 91% with the prior knowledge of the user’s walking path. Ultrasonic distance sensor [27] can identify people with an accuracy between 85% and 95% with the additional help of recording user’s movement. Overall, the performance of our initial designs align with prior work and yet remove the need of cameras or on-body sensors.

6. RELATED WORK

VLC Application. Current VLC applications focus on indoor localization [15, 17, 18, 37], diverse types of communication such as screen-camear communication [2, 8, 10, 11, 21, 30] and LED-to-LED communication [6, 25]. Our work [19] extends VLC applications by using VLC to sense body gestures.

Human Identification. Active research focuses on user identification using either computer vision methods to process video frames, or on-body sensors to capture user behavioral patterns. In particular, Wang et al. [32] extracts body shapes from videos and detects the pattern of several body parts in movement. Wang et al. [33] and Bovick et al. [3] apply statistical methods to extract features from entire body shape. Iwashita et al. [12] exploits histogram to get features in shadow rather than body shape. Kale et al. [13] combines face recognition and gait analysis.

Vu [29] identify differences between users by the behavior of capacitive touch. Hayashi [9] uses Kinect to collect body figures with gestures to identify people. [20, 26] leverage multiple sensors on a smartphone to learn users’ walking behavior. Wang [31] extracts features of walking from video and combine them with smartphone sensors to create personal fingerprint. Furthermore, several advanced sensors are designed for user identification, such as IR sensor [7, 36], ultrasonic sensor [27] and bioimpedance sensor [4].

RF reflections can track multiple people in [14] with bright area on a heatmap of reflected signals, and recognize human activities [5].

In summary, our approach differs from existing methods in that it operates on low-resolution shadow maps without using any cameras, and does not rely on users to constantly wear on-body devices or sensors.

7. CONCLUSION AND FUTURE WORK

In this paper, we present the framework of human identification using the visible light. The system leverage VLC to recover shadows of individual light sources. The shadow maps from different angles help localize key points on human body, thus we can extract key body parameters and leverage them as features for user identification. Preliminary results show that the error of feature estimation is roughly 0.03 m and the identification granularity of body figures is 0.02 m for our current participants. The initial results demonstrates the potential of our approach and yet also point out open research questions we plan to further pursue.

Moving forward, we plan to address the following remaining challenges. First, we plan to examine a greater variety of user movements and examine our initial identification algorithms more extensively with more participants. To do so, we plan to add a glass cover atop all the light sensors in our testbed, which will allow users to move more freely. Second, we plan to incorporate more features into our classifier to achieve finer-grained identification. In particular, we are interested in examining the time series of shadow maps and learn user’s movement characteristics from the shadow map changes over time. Third, with the enriched user features, we plan to examine the feasibility of inferring more user information such as gender, age, and even mood and health status. Fourth, we plan to examine the multi-user scenario where the shadows cast by individual users likely overlap. We aim to seek more advanced algorithms to separate out user shadows and identify individual users.

8. ACKNOWLEDGMENTS

We sincerely thank anonymous reviewers for the constructive comments. We also thank Rui Wang, Xinyun Tang, Peilin Hao and other students for their help on our experiments. This work is supported in part by the National Science Foundation under grant CNS-1421528. Any opinions, findings, and conclusions or recommendations expressed in this material are those of the authors and do not necessarily reflect those of the funding agencies or others.

9. REFERENCES

- [1] ADIB, F., KABELAC, Z., KATABI, D., AND MILLER, R. C. 3D Tracking via Body Radio Reflections. In *Proc. of NSDI* (2014).
- [2] ASHOK, A., ET AL. Challenge: Mobile optical networks through visual MIMO. In *Proc. of MobiCom* (2010).
- [3] BOBICK, A. F., AND JOHNSON, A. Y. Gait recognition using static, activity-specific parameters. In *Proc. of CVPR* (2001), vol. 1, IEEE, pp. 1–423.
- [4] CORNELIUS, C., PETERSON, R., SKINNER, J., HALTER, R., AND KOTZ, D. A wearable system that knows who wears it. In *Proc. of MobiSys* (2014), ACM, pp. 55–67.
- [5] DE SANCTIS, M., CIANCA, E., DI DOMENICO, S., PROVENZIANI, D., BIANCHI, G., AND RUGGIERI, M. WIBECAM: Device Free Human Activity Recognition Through WiFi Beacon-Enabled Camera. In *Proc. of WPA* (2015), ACM, pp. 7–12.
- [6] DIETZ, P., YERAZUNIS, W., AND LEIGH, D. Very low-cost sensing and communication using bidirectional LEDs. In *Proc. of UbiComp*. 2003.
- [7] FANG, J.-S., HAO, Q., BRADY, D. J., GUENTHER, B. D., AND HSU, K. Y. Real-time human identification using a pyroelectric infrared detector array and hidden markov models. *Optics express* 14, 15 (2006), 6643–6658.

- [8] HAO, T., ZHOU, R., AND XING, G. COBRA: Color barcode streaming for smartphone systems. In *Proc. of MobiSys* (2012).
- [9] HAYASHI, E., MAAS, M., AND HONG, J. I. Wave to me: user identification using body lengths and natural gestures. In *Proc. of CHI* (2014), ACM, pp. 3453–3462.
- [10] HU, W., GU, H., AND PU, Q. LightSync: Unsynchronized visual communication over screen-camera links. In *Proc. of MobiCom* (2013).
- [11] HU, W., MAO, J., HUANG, Z., XUE, Y., SHE, J., BIAN, K., AND SHEN, G. Strata: Layered Coding for Scalable Visual Communication. In *Proc. of MobiCom* (2014).
- [12] IWASHITA, Y., AND STOICA, A. Gait recognition using shadow analysis. In *Symposium on BLISS* (2009), IEEE, pp. 26–31.
- [13] KALE, A., ROYCHOWDHURY, A. K., AND CHELLAPPA, R. Fusion of gait and face for human identification. In *Proc. of ICASSP* (2004), vol. 5, IEEE, pp. V–901.
- [14] KATABI, F. A. Z. K. D. Multi-Person Localization via RF Body Reflections. In *Proc. of NSDI* (2015).
- [15] KIM, H.-S., ET AL. An indoor visible light communication positioning system using a RF carrier allocation technique. *Journal of Lightwave Technology* 31, 1 (2013), 134–144.
- [16] KOMINE, T., AND NAKAGAWA, M. Fundamental analysis for visible-light communication system using LED lights. *IEEE Transactions on Consumer Electronics* 50, 1 (2004), 100–107.
- [17] KUO, Y.-S., PANNUTO, P., HSIAO, K.-J., AND DUTTA, P. Luxapose: Indoor positioning with mobile phones and visible light. In *Proc. of MobiCom* (2014), ACM, pp. 447–458.
- [18] LI, L., HU, P., PENG, C., SHEN, G., AND ZHAO, F. Epsilon: A visible light based positioning system. In *Proc. of NSDI* (2014).
- [19] LI, T., AN, C., TIAN, Z., CAMPBELL, A. T., AND ZHOU, X. Human sensing using visible light communication. In *Proc. of MobiCom* (2015).
- [20] LU, H., HUANG, J., SAHA, T., AND NACHMAN, L. Unobtrusive gait verification for mobile phones. In *Proc. of ISWC* (2014), ACM, pp. 91–98.
- [21] PERLI, S. D., AHMED, N., AND KATABI, D. PixNet: Interference-free wireless links using LCD-camera pairs. In *Proc. of MobiCom* (2010).
- [22] POST, E. R., ORTH, M., RUSSO, P. R., AND GERSHENFELD, N. E-broidery: Design and fabrication of textile-based computing. *IBM Systems Journal* 39, 3.4 (2000), 840–860.
- [23] PU, Q., GUPTA, S., GOLLAKOTA, S., AND PATEL, S. Whole-home gesture recognition using wireless signals. In *Proc. of MobiCom* (2013).
- [24] SBÍRLEA, D., BURKE, M. G., GUARNIERI, S., PISTOIA, M., AND SARKAR, V. Automatic detection of inter-application permission leaks in android applications. *IBM Journal of Research and Development* 57, 6 (2013), 10–1.
- [25] SCHMID, S., CORBELLINI, G., MANGOLD, S., AND GROSS, T. R. LED-to-LED visible light communication networks. In *Proc. of MobiHoc* (2013).
- [26] SHI, W., YANG, J., JIANG, Y., YANG, F., AND XIONG, Y. Senguard: Passive user identification on smartphones using multiple sensors. In *Proc. of WiMob* (2011), IEEE, pp. 141–148.
- [27] SRINIVASAN, V., STANKOVIC, J., AND WHITEHOUSE, K. Using height sensors for biometric identification in multi-resident homes. In *Pervasive Computing*. Springer, 2010, pp. 337–354.
- [28] TSONEV, D., ET AL. A 3-Gb/s Single-LED OFDM-based Wireless VLC Link Using a Gallium Nitride μ LED. *Photonics Technology Letters, IEEE PP*, 99 (2014), 1–1.
- [29] VU, T., BAID, A., GAO, S., GRUTESER, M., HOWARD, R., LINDQVIST, J., SPASOJEVIC, P., AND WALLING, J. Distinguishing users with capacitive touch communication. In *Proc. of MobiCom* (2012), ACM, pp. 197–208.
- [30] WANG, A., MA, S., HU, C., HUAI, J., PENG, C., AND SHEN, G. Enhancing Reliability to Boost the Throughput over Screen-camera Links. In *Proc. of MobiCom* (2014).
- [31] WANG, H., BAO, X., ROY CHOUHDURY, R., AND NELAKUDITI, S. Visually fingerprinting humans without face recognition. In *Proc. of MobiSys* (2015), ACM, pp. 345–358.
- [32] WANG, L., NING, H., TAN, T., AND HU, W. Fusion of static and dynamic body biometrics for gait recognition. *Circuits and Systems for Video Technology, IEEE Transactions on* 14, 2 (2004), 149–158.
- [33] WANG, L., TAN, T., HU, W., AND NING, H. Automatic gait recognition based on statistical shape analysis. *Image Processing, IEEE Transactions on* 12, 9 (2003), 1120–1131.
- [34] WANG, Y., LIU, J., CHEN, Y., GRUTESER, M., YANG, J., AND LIU, H. E-eyes: Device-free Location-oriented Activity Identification Using Fine-grained WiFi Signatures. In *Proc. of MobiCom* (2014).
- [35] WEINBERG, Z., CHEN, E. Y., JAYARAMAN, P. R., AND JACKSON, C. I still know what you visited last summer: Leaking browsing history via user interaction and side channel attacks. In *Proc. of IEEE Symposium on Security and Privacy* (2011).
- [36] YUN, J., AND LEE, S.-S. Human movement detection and identification using pyroelectric infrared sensors. *Sensors* 14, 5 (2014), 8057–8081.
- [37] ZHANG, W., AND KAVEHRAD, M. Comparison of VLC-based indoor positioning techniques. In *Proc. of SPIE* (2013).
- [38] ZHOU, X., AND CAMPBELL, A. Visible Light Networking and Sensing. In *Proc. of HotWireless* (2014).